Pore Connectivity, Episodic Flow, and Unsaturated Diffusion in Fractured Tuff

Qinhong Hu [1], Robert P. Ewing [2], Liviu Tomutsa [3], and Michael J. Singleton [1]

[1] *Lawrence Livermore National Laboratory, 7000 East Avenue, Livermore, CA 94550, United States, hu7@llnl.gov*
[2] *Iowa State University, Ames, IA 50011, United States, ewing@iastate.edu*
[3] *Lawrence Berkeley National Laboratory, 1 Cyclotron Road, Berkeley, CA 94720, United States, ltomutsa@lbl.gov*

Abstract – *We use an integrated approach consisting of experiments and complementary pore-scale network modeling to investigate the occurrence of sparsely connected pore spaces in rock matrices at Yucca Mountain, Nevada, and their implications for matrix diffusion. Imbibition results indicate that pore spaces in devitrified tuff are not well-connected, and that this lack of connectivity is further compounded by episodic flow in fractured devitrified tuff with low matrix permeability. A rigorous methodology for investigating chemical transport in fractured rock under episodic conditions, employing a suite of both sorbing and non-sorbing tracers (including radionuclides U-235, Np-237, and Pu-242), has been developed and implemented. In addition, gas diffusion and synchrotron microtomography techniques have been under development to examine the scaling issues of diffusion and pore connectivity. Preliminary results from experiments and modeling work are presented in this paper, confirming the need to reexamine our understanding of matrix diffusion and to evaluate the impact on diffusive radionuclide retardation of episodic fracture flow and low pore connectivity.*

I. INTRODUCTION

Current models of how radionuclide movement is slowed by diffusion into and sorption to the rock matrix do not consider two potentially important factors. First, some Yucca Mountain tuffs have a sparsely connected pore space, resulting in scale-dependent diffusion—but models currently use a constant diffusion term. Second, under episodic and intermittent flow in the unsaturated zone, the rock matrix is constantly imbibing or draining water, which drives advective movement of radionuclides while changing the effective diffusivity of the matrix—but site-scale models currently assume constant wetness conditions.

It was recently shown [1-2] that Yucca Mountain devitrified welded tuff is not well interconnected at the pore scale, meaning that standard diffusion models can yield incorrect values for measured and predicted diffusion, and thereby retardation rates [3]. These results are consistent with both experimental work on diffusion at low phase saturations [4], and theoretical work that shows how diffusion at low phase saturations and/or pore connectivity can be characterized as a percolation problem [5]. Use of a percolation paradigm for diffusion suggests both specific mathematical tools for up-scaling from laboratory to in-situ scales, and the use of a pore-scale random walk modeling approach to help understand and interpret the experiments.

Orographic effects cause substantial variability in average annual precipitation at Yucca Mountain, ranging from <130 mm at the low elevations in the south to >200 mm in the north, with an average annual precipitation of 170 mm [6]. Bodvarsson et al. [7] indicate that infiltration at Yucca Mountain is spatially and temporally variable due to the nature of storm events, variations in soil cover and topography. Significant infiltration occurs only every few years. In these wet years, the amount of infiltration still varies greatly because it is dependent on storm amplitudes, durations, or frequencies; infiltration pulses on the order of hundreds of millimeters per year may infiltrate into Yucca Mountain during relatively short periods of time.

Because of the spatially and temporally variable nature of infiltration, water percolation through unsaturated fractured rocks of low matrix permeability is episodic and intermittent in nature [8]. Infiltration pulses may be attenuated by the Paintbrush non-welded (PTn), a unit above the potential geological repository with very limited fracturing, such that liquid-water flow below the PTn is considered to be approximately in steady state. However, bomb-pulse isotopes data provide strong evidence of fast pathways through the unsaturated zone to the level of the potential repository underlying the breaks in the PTn [9]. The locations most likely to have fast pathways are those where the inter-layered, non-welded tuff is faulted, absent, or very thin. Simulations of transient flow and transport at Yucca Mountain using a dual continuum model [10] indicate that rapid movement of solute through the fractures will occur only in the event of intense infiltration episodes.

With episodic flow varying in rate and intensity, the matrix is constantly imbibing or drying, and this fluctuating wetness both drives two-way advective movement of radionuclides, and forces changes in the matrix diffusivity. To date, measurements and models have all assumed classical, steady-state diffusion, without testing the validity of that assumption. The ultimate

effect on radionuclide migration and retardation, of wetting and drying cycles coupled with low pore connectivity, has never been examined, despite it being fundamental to the processes at Yucca Mountain. The objectives of this work are to reexamine our understanding of matrix diffusion, to provide insights into up-scaling laboratory-scale diffusion experiments, and to evaluate the impact on diffusive radionuclide retardation of episodic fracture flow and low pore connectivity.

II. EXPERIMENTAL AND MODELING WORK

We acquired 21 samples from boreholes UE-25 UZ#16, USW SD-9, and USW SD-12, representing all unsaturated zone layers between the potential repository and the water table: Topopah Spring devitrified (middle nonlithophysal, lower lithophysal, and lower nonlithophysal zones), and Calico Hills vitric (CHv) and zeolitic (CHz) tuff. With a wide range of porosity (0.036 − 0.345) and saturated hydraulic conductivity (4.0×10^{-11} – 1.6×10^{-5} m/s) reported for these tuffs [11], along with various degree of welding, mineralogy, and diagenetic alteration (zeolitization), it is expected that they will exhibit different degrees of pore connectivity, and therefore, affect imbibition and diffusion processes differently.

Complementary, integrated and innovative experimental/modeling approaches are pursued to achieve the research objectives stated above. These approaches include imbibition (analogous to diffusion, but easier to conduct because of its shorter experimental duration) tests on samples of different height:diameter ratios (i.e., shape), gas diffusion experiments at several different sample thicknesses to examine scaling effects, fracture flow and tracer transport tests with 4 episodes of liquid release, with micro-scale (laser ablation interfaced with inductively coupled plasma-mass spectrometry, LA/ICP-MS) measurements of tracer distribution on the rock sample [12], synchrotron microtomography imaging at the Advanced Light Source (ALS) of LBNL, and pore network modeling using random walks on 3-D lattices with different pore coordination and connectivity. All these approaches are targeted to study the interacting processes of diffusion, imbibition, and sorption of radionuclides, as affected by pore connectivity and the episodic nature of flow in unsaturated fractured tuff at Yucca Mountain.

II.A. Liquid Imbibition

Imbibition tests involved exposing one face of a rock sample to water (or tracer solution), and monitoring the water uptake rate over time. For tracer imbibition and transport, we used a mixture of nonsorbing and sorbing tracers, designed to mimic the principle radionuclides in the Yucca Mountain inventory, and examined their penetration distance during imbibition. The slope of log imbibed water mass versus log time is indicative of the pore connectivity [1]. The pore-scale network model indicates that the slope will be ½ at a high (>0.28) value of p (the mean probability of connectivity) and 0.26 (~1/4) at p=0.249 (the percolation threshold). At intermediate values (p≈0.255), corresponding to poorly connected pore spaces, the slope transitions from ¼ to ½ at some time or distance from the imbibing surface. In other words, just above the percolation threshold, solute diffusion (analogous to water imbibition) is anomalous at short times and distances, and later assumes "normal" (Fickian) long-term behavior. The distance to the wetting front at this crossover point corresponds to the correlation length of percolation theory.

A bottom-weighing (for hanging the rock sample) analytical balance with a resolution of 0.1 mg is used to measure the sample weight change during liquid imbibition. Free logging software, Windmill LabIML 4.3 (Windmill Software Ltd, Manchester, UK; http://www.windmill.co.uk/), was set up to log the balance readings to a computer at selected time intervals, starting with every second at the begining of imbibition and increasing over time); visual verification has confirmed the desired function of the software. Core samples of varying height:diameter ratios were used to investigate the shape effect.

In order to characterize pore connectivity in 10 UZ model layers (TSw34 to 39, vitric subzone ch1, zeolitized ch1, vitric ch2-5, and zeolitized ch2-5) below the potential repository at Yucca Mountain, we conducted replicate measurements of water imbibition into initially dry tuff samples of several shapes. For Topopah Spring welded tuff (TSw34), vitric Calico Hills (CHv), and zeolitized Calico Hills (CHz) samples – the major tuff types with different mineralogy and chemical reactivity – we also performed tracer imbibition and tracer transport tests into initially dry samples of TSw, CHv, and CHz.

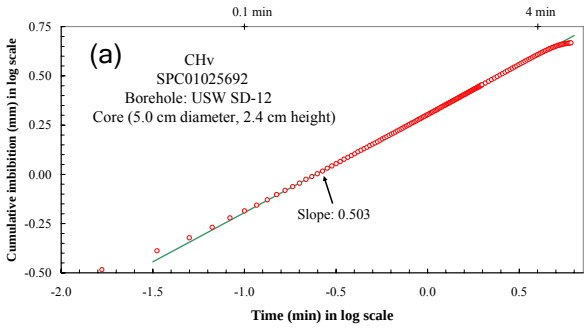

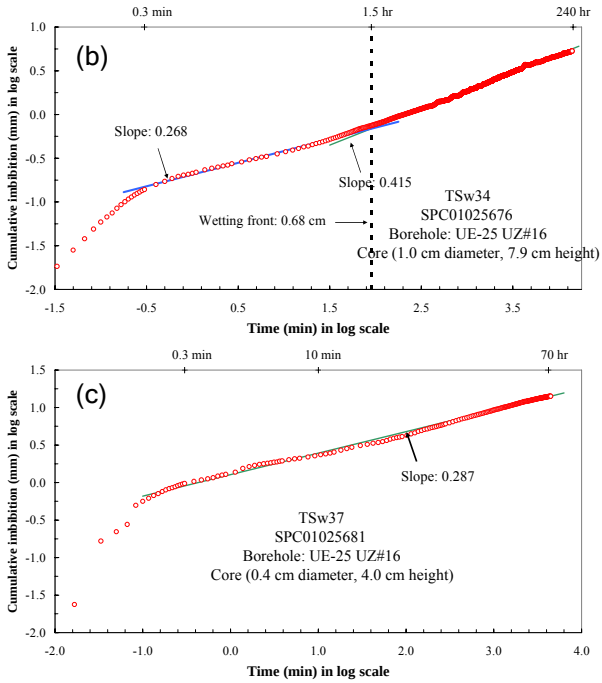

Figure 1. Water imbibition into tuffs with three types of imbibition slopes; (a) ½ slope; (b) ¼ transitioning to ½ slope; and (c) ¼ slope.

Three different imbibition slope behaviors were seen as a result of different pore connectivities (Figure 1). In devitrified rock, slopes are sensitive to the sample's shape, with tall thin samples being more likely to have a slope of ¼ (anomalous diffusion behavior), sometimes followed by crossover to a slope of ½ (classical). Short squat samples never display ¼-type behavior. These results confirm that the devitrified rock pore space is sparsely connected. Conversely, vitric and zeolitic Calico Hills tuff likely has well connected pore spaces, with the imbibition slopes showing only the ½-type behavior.

II.B. Gas Diffusion Measurement

To investigate the effect of scaling on diffusive transport in Yucca Mountain tuff, we will measure gas diffusion coefficients for Yucca Mountain tuff, using samples of several lengths. The system for measuring gas diffusion in consolidated rock takes advantage of a rapid mass spectrometric technique. The Membrane Inlet Mass Spectrometry (MIMS), custom- built at LLNL based on a design by Kana et al. [13], has a large dynamic measurement range of several orders of magnitude, rapid data acquisition, and continuous real-time data display. Gas concentration is continuously monitored during the experiment, which takes only minutes because of the larger (nearly four orders of magnitude) diffusivity of gases than liquids.

We have started testing the setup and procedure using both no rock sample (i.e., empty copper tube) to obtain the base case of gas diffusion in air, and a sample of the reference rock, Berea sandstone. Two diffusing gases (helium and sulphur hexafluoride, SF_6) with different diffusion coefficients were employed to assure that only diffusion is operative (i.e., no or minimal effect of advection). Gas concentration of these tracers (as well as nitrogen and argon in the air) was continuously monitored using the MIMS. Figure 2 shows an example of diffusive transport of two gases under pulse release in the Berea Sandstone core (1cm diameter and 3 cm long), with SF_6 exhibiting later breakthrough (i.e., slower diffusion) because its gas diffusion coefficient in air (7.7×10^{-6} m^2/s) is lower than that of He (5.8×10^{-5} m^2/s). The developed techniques will be used to measure gas diffusion coefficients for two Yucca Mountain tuffs (Topopah Spring devitrified, Calico Hills zeolitic) of several lengths; unfortunately the CHv sample is too friable to permit coring a long (>3 cm) sample.

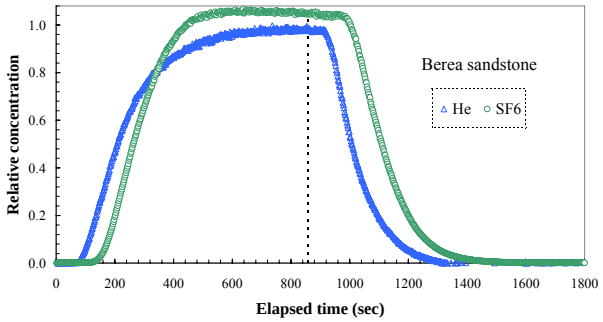

Figure 2. Diffusive transport of gaseous tracers in Berea sandstone. The vertical line indicates the time when the tracer gas release was stopped.

II.C. Synchrotron Microtomography

We imaged a dry TSw34 tuff core (4 mm diameter, 40 mm in length) using the microtomography beamline 8.3.2 of the Advanced Light Source at LBNL. The energy used was 35 keV, just above the iodine K edge; this maximizes sensitivity to the iodine tracer used in the diffusion test. A total of 35 scans, each 200 pixels high, was taken to cover the entire length of the sample. The camera used, an Apogee KAF1602e, has a resolution of 1536×1024 pixels with a 14 bits/pixel well depth, each pixel being 6 microns in size. The images show that the sample presents micron-scale heterogeneity (Figure 3), which will be considered in the interpretation of future diffusion results. The higher resolution (3072×2048 pixels) Quantix KAF6303E camera, being repaired when these images were taken, will enable us to resolve sample heterogeneity at 1.6 micron/pixel resolution.

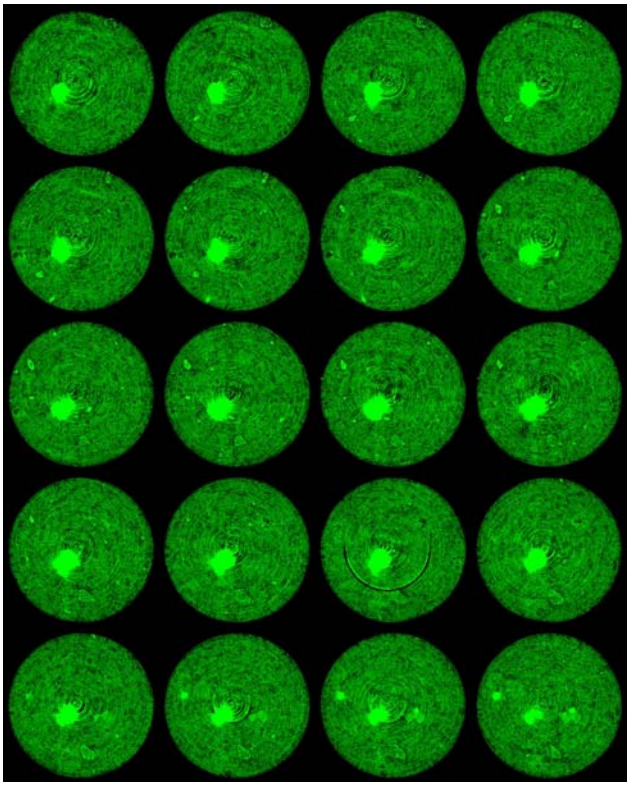

Figure 3. Synchrotron microtomography images taken 30 microns apart; the sequence is from left to right and top to bottom. The bright region strongly attenuates X-rays, so it may contain iron-based minerals such as pyrite and/or calcium minerals such as calcite.

At 33.5 keV, we have also imaged the dry Berea sandstone, which is known to have a well-connected pore space. The 3-D image (Figure 4) measures 248×248×248 voxels, each 4.45 microns in length. Several programs, including Imgrec from LLNL, ImageJ from NIH, and T3D from RSI Inc., were used to process the data.

We have also been testing and refining our experimental approach for microtomography diffusion tests. A sample holder for the diffusion test has been designed and machined. The test will generate 3-D maps of tracer (iodide) concentration over time within the tuff samples. Tracer iso-concentration surfaces will give information on pore connectivity and cross-over length. We have prepared core sample of TSw34, 4mm in diameter and 40mm long. Using the Quantix KAF6303E camera, we expect to get 3-D images with a resolution of a few microns. The TSw core sample was fully saturated with 1 M KCl; in the experiment KCl is replaced by an equal concentration of KI, with iodide having much greater X-ray attenuation than chloride. The sample was imaged vertically, but was in a horizontal position during the diffusion experiment. A 1.2 ml/hr KI solution flow rate was maintained to flush the sample end exposed to KI, ensuring a constant-concentration boundary. The core samples were to be imaged at several time intervals (e.g., at 1, 2, 5, 10, 20, and 60 days' diffusion time). Unfortunately, some logistics and instrumentation issues with the ALS allowed imaging only after 3 months of diffusion, at which time the iodide diffusion concentration was observed to be constant through the entire sample.

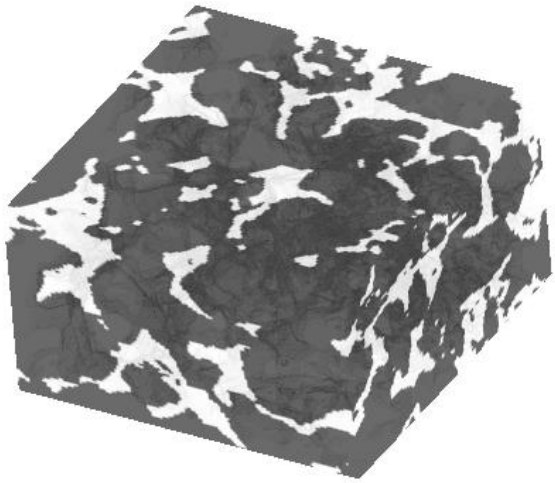

Figure 4. 3-D (1.1 mm each side) image of Berea sandstone. The pore space is white and the grains dark.

In the near future, we will image and process dry tuff samples to examine the pore connectivity (compared to Berea sandstone), as well as the distribution of diffusing iodide inside.

II.D. Episodic Fracture Flow

We first performed a non-episodic flow experiment for comparison, using a TSw34 core (10.2cm length, 4.4cm diameter) with the saw-cut fracture having an aperture of 100 μm. The dry core was packed into a flow reactor, flushed with CO_2, then saturated via slow pumping (0.01 mL/min) of synthetic groundwater. The fractured core was then flushed with air at >97% relative humidity to simulate *in situ* conditions in unsaturated fractured rock at Yucca Mountain, after which the transport experiment was conducted. The tracer solution included ^{3}H, Br^-, ReO_4^- (an analog for $^{99}TcO_4^-$), I^-, Sr, Cs (for $^{129}I^-$, ^{90}Sr, ^{137}Cs), and Sm^{+3} (an analog for actinides with +3 valance state), plus the radionuclides ^{235}U, ^{237}Np, and ^{242}Pu. These tracers span a variety of sorption strengths and represent many of the radionuclides of concern. ^{3}H, Br^-, I^-, and ReO_4^- serve as nonsorbing tracers with different diffusion coefficients. A total of 100 fracture pore volumes of solution were directly released into the fracture to study the worst-case scenario, then the core was flushed with tracer-free synthetic groundwater. Liquid effluent from the flow reactor was continuously

collected for multi-elemental analyses using ICP-MS, as well as liquid scintillation counting for ^{3}H, to obtain the breakthrough curves of non- or less-retarded tracers. To minimize the evaporation effect of effluent samples from such slow flow tests, the fraction collection is placed inside a closed container that maintains a high relative humidity. At the end of the experiment, the distribution of strongly retarded tracers within the core was characterized by the new micro-scale sampling technique of LA/ ICP-MS (Figure 5). While fast transport and early breakthrough are observed, matrix diffusion and imbibition retarded overall chemical transport, as evidenced by long tailing of the nonsorbing tracers (^{3}H, Br^{-}, I^{-}, and ReO_4^{-}) in the elution portion (Figure 5a). Concomitant with the same breakthrough, the strongly-sorbing tracers (Cs, Sm, and ^{242}Pu) were sorbed and retarded on the fracture face within the first 0.5 cm from the injection side (Figure 5b).

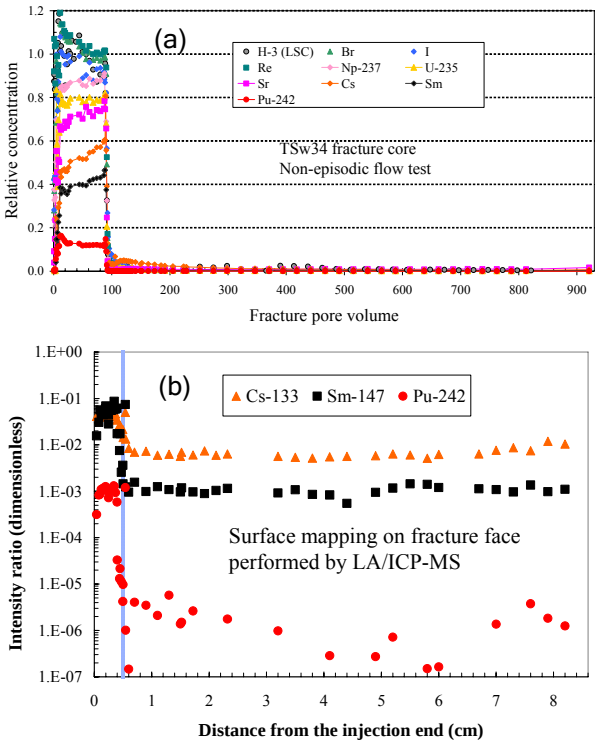

Figure 5. Radionuclide transport in a fractured core column. (a) Effluent breakthrough curves; (b) Distribution of strongly sorbing tracers on the fracture face of the rock.

In contrast to the non-episodic test, the episodic flow and transport test involved 4 cycles of tracer solution flow within the fracture, each followed by flushing with high humidity air. Each flow episode contained at least one nonsorbing and one sorbing tracer. Both liquid and solid samples were analyzed (data currently being processed) to obtain the effluent breakthrough curves and sorbing tracer distribution on the fracture face and the neighboring tuff matrix.

II.E .Pore-Scale Network Modeling

The imbibition process is simulated using a random walk technique developed by Hu and Ewing [1], who found that it reproduced the experimental sensitivity to connectivity of the rock matrix. Imbibition experiments are currently being modeled using 6-connected pore-scale networks measuring 128^3 pores. We had hoped to work with larger networks, but found that doubling the network size in all dimensions increased simulation run time by a factor of 150−200, such that some critical simulations would require more than a full year. Novel speed-up techniques enable us to use networks measuring 256^3 pores for some simulations.

Simulations to date have focused on antecedent water content and matrix connectivity as they affect the time progression of imbibition. Like the imbibition experiments (Figure 1), the simulations show a rapid initial stage where viscosity is not limiting (Figure 6). As expected, imbibition proceeds more rapidly into samples with higher connectivity and lower initial water content. At lower connectivity, imbibition often has two stages: an initial low-slope stage, then a second stage with a slope close to ½ in log-log space. At higher initial saturations the data are noisier, and distinguishing between the two stages is more difficult. Despite this, we see a modest trend toward higher initial slopes in initially wetter media.

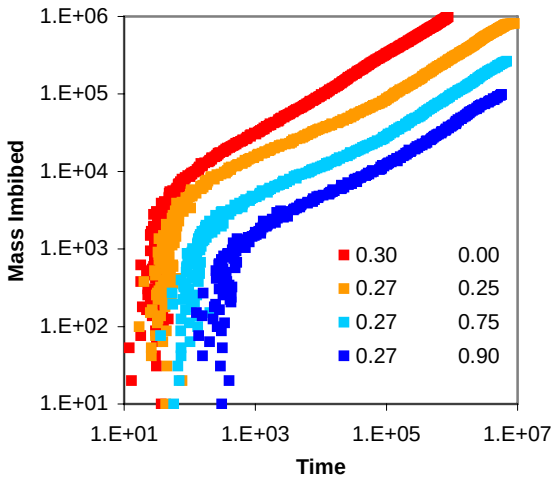

Figure 6. Example simulations of cumulative imbibition over time for one dry, well-connected lattice, and three poorly connected lattices at different initial saturations. Columns in the legend are connectivity and initial saturation, respectively.

We are now using a modified imbibition algorithm that runs much faster while giving results similar to those of the original internal-DLA (diffusion-limited

aggregation) algorithm. Current tests are focused on effects of sample shape and pore connectivity on the simulated imbibition, with the aim of better establishing under what conditions imbibition will proceed in one or two distinct stages. The main difficulty at the moment is working out an objective criterion for determining whether a given imbibition experiment has one or two stages: this issue is more difficult than expected. A new approach, using a hidden Markov model and several information criteria, appears to have promise in resolving this difficulty.

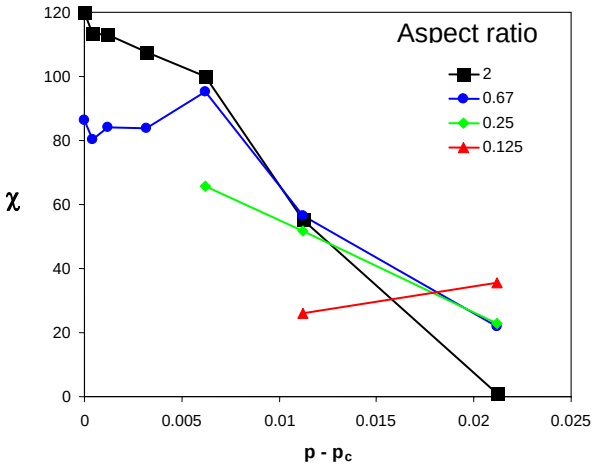

Figure 7. Distance to slope cross-over point χ as a function of connectivity probability above the percolation threshold, and sample aspect ratio (width/height). Because thin (low aspect ratio) samples do not percolate at low values of p-p_c., there are no data for low aspect ratio, low-connectivity simulations.

In accordance with theory, χ (distance to slope cross-over) is greater at lower connectivities. This effect is moderated by sample shape; high aspect ratio samples are more likely to percolate even at low connectivities, whereas few low aspect ratio samples percolate at all (Figure 7). This is consistent with the experimental imbibition results.

As a sample gets relatively wider, the occurrence likelihood of two-stage imbibition decreases (Figure 8). Well-connected samples are less likely to show two stages at any sample shape.

Future modeling work will add advection and sorption to the existing diffusion model, allowing simulation of the episodic flow experiments. Of particular interest is the relationship between the time required for various contaminants to diffuse a distance χ from the fracture, and a "typical" time between infiltration episodes.

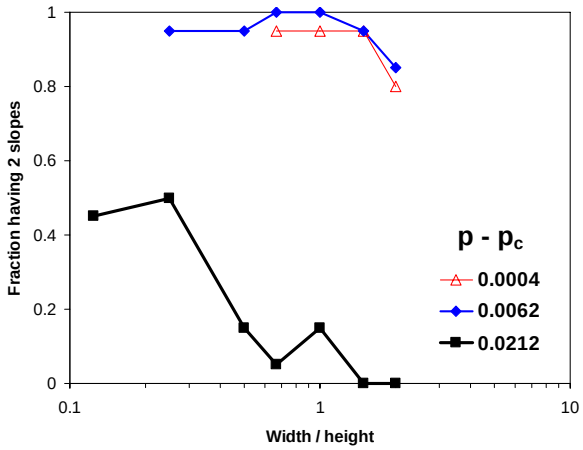

Figure 8. Fraction of realizations having two distinct slopes in their simulated imbibition curve.

III. CONCLUSIONS

This research integrates newly developed experimental and modeling methods, and this paper presents the preliminary results of ongoing work. Results from water imbibition confirm that the pore space in devitrified rock at Yucca Mountain, where the waste packages may potentially be emplaced, is sparsely connected. Use of standard diffusion models to describe matrix diffusion in the densely fractured devitrified tuff matrices can potentially yield misunderstanding of the diffusion process, and thus incorrectly calculated diffusivity values. Results from the fracture tracer transport test indicate that the interacting processes of imbibition, diffusion, and sorption all contribute to radionuclide retardation under fracture-dominated preferential flow.

Overall results from this research work will address uncertainties regarding how pore connectivity, changes in saturation, and episodic flow affect diffusive retardation of radionuclides. This will help to resolve questions central to fracture/matrix interactions and their impact on total repository performance for the potential geological repository at Yucca Mountain.

ACKNOWLEDGMENTS

This work was supported by the United States Department of Energy (DOE), Office of Civilian Radioactive Waste Management (OCRWM), Office of Science and Technology and International (OST&I). This work was performed under the auspices of the U.S. Department of Energy by University of California, Lawrence Livermore National Laboratory under Contract W-7405-Eng-48, and Lawrence Berkeley National Laboratory under Contract DE-AC03-76SFOO098.

REFERENCES

1. Q. HU and R.P. EWING. “Pore connectivity effects on solute transport in rocks”. Bridging the Gap Between Measurement and Modeling in Heterogeneous Media. Proceedings of the International Groundwater Symposium, Berkeley, California (2002).
2. Q. HU, T.J. KNEAFSEY, R.C. TRAUTZ, and J.S.Y. WANG. “Tracer penetration into welded tuff matrix from flowing fractures”, *Vadose Zone J.*, **1**, 102-112 (2002).
3. R.P. EWING and R. HORTON. “Diffusion in sparsely connected pore spaces: Temporal and spatial scaling”. *Water Resour. Res.*, **38**, 1285, doi:10.1029/2002WR001412 (2002).
4. P. MOLDRUP, T. OLESON, T. KOMATSU, P. SCHJONING, and D.E. ROLSTON. “Tortuosity, diffusivity, and permeability in the soil liquid and gaseous phases”. *Soil Sci. Soc. Am. J.*, **65**, 613–623 (2001).
5. A. G. HUNT and R. P. EWING. On the vanishing of solute diffusion in porous media at a threshold moisture content. *Soil Sci. Soc. Am. J.*, **67**, 1701 (2003).
6. A. L. FLINT, L. E. FLINT, E. M. KWICKLIS, G. S. BODVARSSON and J. M. FABRYKA-MARTIN. “Hydrology of Yucca Mountain, Nevada”. *Rev. Geophy.*, **39**, 447-470 (2001).
7. G.S. BODVARSSON, W. BOYLE, R. PATTERSON and D. WILLIAMS. “Overview of scientific investigations at Yucca Mountain - the potential repository for high-level nuclear waste”. *J. Contam. Hydrol.*, **38**, 3-24 (1999).
8. K. PRUESS. “A mechanistic model for water seepage through thick unsaturated zones in fractured rocks of low matrix permeability”. *Water Resour. Res.*, **35**, 1039-1051 (1999).
9. K. CAMPBELL, A. WOLFSBERG, J. FABRYKA-MARTIN and D. SWEETKIND. “Chlorine-36 data at Yucca Mountain: Statistical tests of conceptual models for unsaturated-zone flow”. *J. Contam. Hydrol.*, **62-3,** 43-61 (2003).
10. R.G. MCLAREN, P.A. FORSYTH, E.A. SUDICKY, J.E. VANDERKWAAK, F.W. SCHWARTZ and J.H. KESSLER. “Flow and transport in fractured tuff at Yucca Mountain: Numerical experiments on fast preferential flow mechanisms”. *J. Contam. Hydrol.*, **43**, 211-238 (2000).
11. L.E. FLINT. “Physical and hydraulic properties of volcanic rocks from Yucca Mountain, Nevada”. *Water Resour. Res.*, **39**, 1119, doi:10.1029/2001WR001010 (2003).
12. Q. HU, T.J. KNEAFSEY, J.S.Y. WANG, L. TOMUTSA, and J.J. ROBERTS. “Characterizing unsaturated diffusion in porous tuff gravels”. *Vadose Zone J.*, **3**,1425-1438 (2004).
13. T.M. KANA, C. DARKANGELO, M.D. HUNT, J.B. OLDHAM, G.E. BENNETT, and J.C. CORNWELL. “Membrane inlet mass spectrometer for rapid high-precision determination of nitrogen, oxygen, and argon in environmental water samples”. *Anal. Chem.*, **66**, 4166-4170 (1994).